International Journal of ChemTech Research
CODEN (USA): IJCRGG ISSN: 0974-4290
Vol.7, No.01, pp 460-473, 2014-2015

Density functional theory, restricted Hartree-Fock simulations and FTIR, FT-Raman and UV-Vis spectroscopic studies on Metronidazole

S. Harikrishnan* and T.J.Bhoopathy

PG and Research Department of Physics, Pachaiyappa's College,Chennai- 600030, Tamilnadu, India

Abstract: The FTIR and FT-Raman spectra of metronidazolewere recorded in the regions 4000-400cm^{-1} and 4000-400cm^{-1}respectively. The spectroscopic data of the molecule in the ground state were calculated using Hartee-Fock and Density Functional Method (B3LYP) with 6-31G(d,p) basis set. With the observed FTIR and FT-Raman data, a complete vibrational band assignment and analysis of the fundamental modes of the compound were carried out. Thermodynamic properties and atomic charges were calculated using both Hartee-Fock and Density Functional Method using theB3LYP/6-31G(d,p) basis set and compared. The calculated HOMO-LUMO energy gap revealed that charge transfer occurs within the molecule.^{1}H and ^{13}C NMR chemical shifts of the molecule were calculated using Gauge Including Atomic Orbital (GIAO) method and were compared with experimental results.
Key Words: Metronidazole, FTIR, NMR, HOMO-LUMO.

1. Introduction

5-Nitroimadazoles Such as Metronidazole are extensively used as antiamoebic, antiprotozoal, antibiotic and antibacterial drugs. The discovery of the antibacterial and antitrichomonal properties of the antibiotic azomycin led to the investigation of nitroimidazoles as antiparasitic agents [1,2]. Nitroimidazole derivatives presents biological activity against anaerobic micro-organisms, being largely used as active ingredient of antihelminthic medicine [3]. The discovery of the antitrichromal properties of metronidazole revolutionized the treatment of disease. The properties of metronidazole were studied; it was not clinically tested until some years later. In laboratory tests, Metronidazole is effective against intestinal amoebiasis in rats and hepatic amoebiasis in hamsters and also active against Entamoeba histolytica in vitro [4].The initial clinical tests of metronidazole indicated that it was capable of Curing invasive amoebic dysentery and amoebic liver abscess [5]. Subsequent clinical tests have established metronidazole as the drug of choice in the treatment of all forms of amoebiasis in humans [6, 7]. Metronidazole is officially determined by titrimetry, potentiometry and HPLC methods. Indian Pharmacopoeia [8] describes the non-aqueous titration method using Perchloric acid as titrant and malachite green as indicator for the assay of metronidazole. British Pharmacopoeia [9] describes potentiometric and non-aqueous methods using perchloric acid as titrant. United states Pharmacopoeia [10] describes HPLC and non aqueous titration methods for the assay of metronidazole. Several methods have been reported for the determination of metronidazole including Spectrophotometry [11-13] and Polarograpy[14].

2. Experimental

Metronidazole with >99% purity was obtained from Chennai reputed company, Chennai and was used without further treatments. The FTIR spectrum of the powder sample was recorded in KBr in the range 4000 – 400 cm^{-1} using a Perkin Elmer spectrometer with a resolution of ±1 cm^{-1}. FT- Raman spectrum of the powder sample was recorded using 1064 nm line Nd:YAG laser as the excitation wavelength in the region 4000-50 cm^{-1} using Bruker RFS 27 spectrometer. The UV–Vis spectrum was recorded in the range 200-900nm using a Varian

Cary 5E-UV-NIR spectrophotometer. ^{1}H and ^{13}C Nuclear Magnetic Resonance (NMR) spectral measurements were recorded with Bruker AVANCE III 500 MHz. All spectral measurements were carried out at Sophisticated Analytical Instrument Facility, IIT Madras, India.

3.Computational Details

To provide complete information regarding the structural characteristicsand the fundamental vibrational modes of Metronidazole, the Restricted Hartree-Fock and DFT-B3LYP correlation functional calculations have been carried out. The calculationsof geometrical parameters in the ground state were performed using Gaussian 03programs [15], invoking gradient geometry optimization [16] on Intel core i4/2.93 GHz processor.The computations were performed at RHF/6-31G(d,p), B3LYP/6-31G(d,p) levels to obtain the optimized geometrical parameters, vibrational wavenumbers of the normal modes, IR intensity, atomic charges and thermodynamical parameters of the compound. DFT calculations were performed using Becke's three-parameter hybrid model using Lee-Yang-Parr (B3LYP) correlation function method.

3. Results and Discussion

4.1 Molecular geometry

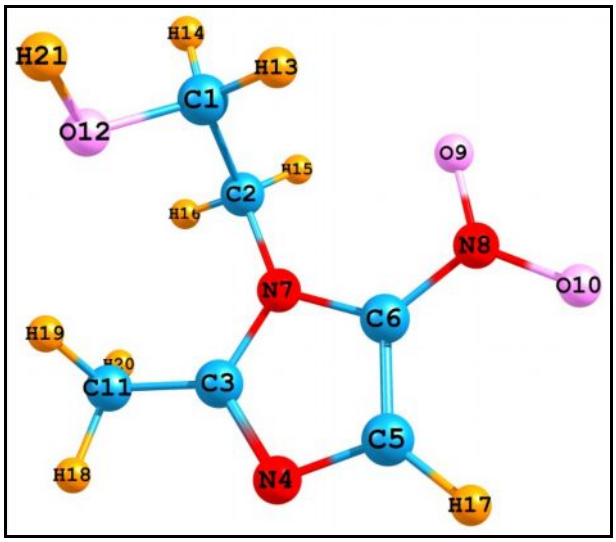

Fig 1. Optimized molecular structure and atomic numbering of Metronidazole

The molecule Metronidazole has 21 atoms with 57 normal modes of vibration. It belongs to the C_1 point group symmetry. Fig. 1 shows the optimized geometry of the molecule and Table 1 presents the optimized values obtained for bond lengths and bond angles. The various bond lengths and bond angles are found to be almost same at RHF/6-31G (d,p)and B3LYP/6-31G(d,p) methods. The bond length between C1-C2 in RHF and B3LYP method are found to be 1.517 and 1.523respectively, which are in good agreement with the experimental value 1.5230. The bond length between C2 and N7 in RHF and B3LYP are 1.462 and 1.468 respectively. The B3LYP value is in good agreement with the experimental value of 1.470. The bond angle between C1-C2-H16 in RHF and B3LYP are 109.1° and 109.5°respectively, and the corresponding experimental value is 109.4620°. The bond angle between N7-C6-N8 in RHF and B3LYP are 125.9° and 125.7° respectively and the corresponding experimental value is 124.6395°. The experimental values [17] are in good agreement with values based on B3LYP method.

Table 1: Experimental values and theoretically optimized geometrical parameters of Metronidazole obtained by RHF/6-31G(d,p) and B3LYP/6-31G(d,p) methods

Structural parameters	RHF	B3LYP	Expt.
Bond length			
C1-C2	1.517	1.523	1.5230
C1-O12	1.402	1.422	1.4020
C1-H13	1.084	1.097	1.1130
C1-H14	1.089	1.101	1.1130
C2-N7	1.462	1.468	1.4700
C2-H15	1.077	1.088	1.1130
C2-H16	1.08	1.092	1.1130
C3-N4	1.309	1.334	1.3659
C3-N7	1.345	1.366	1.3131
C3-C11	1.494	1.492	1.4970
C4-C5	1.345	1.355	1.3674
C5-C6	1.356	1.381	1.3746
C5-H17	1.069	1.08	1.1000
C6-N7	1.385	1.393	1.3709
C6-N8	1.41	1.416	1.2480
N8-O9	1.203	1.243	1.3100
N8-O10	1.195	1.234	1.3100
C11-H18	1.08	1.09	1.1130
C11-H19	1.082	1.093	1.1130
C11-H20	1.086	1.097	1.1130
O12-H21	0.942	0.965	0.9420
Bond angle			
C2-C1-O12	108.1	108.1	109.4996
C2-C1-H13	109.9	109.1	109.4416
C2-C1-H14	108.1	107.9	109.4618
C1-C2-N7	112.8	112.9	109.4998
C1-C2-H15	110.1	109.6	109.4419
C1-C2-H16	109.1	109.5	109.4620
O12-C1-H13	111.6	112.2	109.4420
O12-C1-H14	111.1	111.6	109.4619
C1-O12-H21	110.3	108.6	119.9993
H13-C1-H14	108.1	107.9	109.5204
N7-C2-H15	108.9	108.6	109.4417
N7-C2-H16	107.1	107.1	109.4617
C2-N7-C3	125.9	125.9	127.3472
C2-N7-C6	129.3	128.9	127.3472
H15-C2-H16	108.6	109.1	109.5202
N4-C3-N7	112.7	112.2	111.4781
N4-C3-C11	123.1	123.9	124.2608
C3-N4-C5	106.1	106	107.4787
N7-C3-C11	124.2	123.9	124.2611
C3-N7-C6	104.7	105.3	105.3056
C3-C11-H18	107.8	107.9	109.5001
C3-C11-H19	111	111	109.4419
C3-C11-H20	111.1	111.8	109.4619
N4-C5-C6	109.5	109.9	105.0162
N4-C5-H17	123.1	123.2	127.4918
C6-C5-H17	127.3	126.8	127.4920
C5-C6-N7	106.9	106.6	110.7214

C5-C6-N8	127.1	127.6	124.6390
N7-C6-N8	125.9	125.7	124.6395
C6-N8-O9	118.7	118.9	119.9997
C6-N8-O10	116.9	116.9	120.0002
O9-N8-O10	124.4	124.2	120.0001
H18-C11-H19	109.7	109.7	109.4418
H18-C11-H20	108.5	108.3	109.4619
H19-C11-H20	108.6	108.2	109.5198

4.2 Vibrational analysis

The observed and calculated frequencies using RHF/6-31G(d,p) and B3LYP/6-31G(d,p) methods and their IR intensities and assignments are listed in Table 2. Experimental FTIR, theoretical FTIRandexperimental FT-Raman spectra of Metronidazole are shown in Figs. 2, 3 and 4 respectively.The description of band assignments isas follows.

Table 2 The observed and calculated frequencies of Metronidazole using RHF/6-31G(d,p)and B3LYP/6-31G(d,p)methods

Experimental		Theoretical				Vibrational Assignments
FTIR	FT-Raman	RHF		B3LYP		
		Frequency	Intensity	Frequency	Intensity	
3819	4385	4196	73.2	3840	0.1	OH υ (100)
3420	3411	3456	0.3	3283	2.5	CH υ (99)
	3208	3347	3.9	3177	1.4	CH_2 asy υ (99)
		3321	4.6	3170	3.4	CH_2 sym υ (98)
		3282	32.5	3120	6.0	CH υ (98)
		3278	8.8	3110	7.6	CH υ (95)
	3065	3250	23.7	3070	17.1	CH υ (87)
	2955	3201	15.5	3048	94.0	CH υ (99)
	2884	3177	66.6	3002	5.7	CH υ (100)
		1820	513.3	1605	4.2	ONυ (76) + CCυ (10)
		1738	82.2	1561	3.6	NCυ (19) + CCυ (18) + HCN b (10)
		1675	119.6	1535	2.7	HCH b (69) + HCCNτ (12)
1646		1661	27.4	1520	3.7	CCυ (32) + HCHb (15)
		1653	172.5	1512	15.1	NCυ (21) + CCυ (18) + HCHb (18)
		1632	320.7	1498	4.3	HCH b (71) + HCCNτ (15)
		1617	14.1	1483	0.8	HCH b (68) + HCNCτ (10)
		1611	85.5	1470	3.3	NCυ (11) + HCH b (25)
		1600	35.3	1456	7.5	HOC b (22) + HCH b (21) + HCCNτ (14)
	1571	1587	70.5	1428	4.6	NCυ (30) + HCH b (11)
		1543	7.7	1408	10.1	ONυ (10) + HCHb (36)
		1532	26.0	1402	27.5	HCHb (15) + HCNCτ (49)
1391	1382	1505	41.0	1394	14.2	NCυ (25) + HCN b (29) + CCN b (11)
		1431	44.3	1312	10.4	NCυ (15) + HCO b (10)
		1417	124.9	1310	4.8	NCυ (20) + HOC b (10)
		1382	14.4	1270	5.0	HOC b (13) + HCO b(27) + HCCNτ (47)
		1332	63.8	1229	4.8	HOC b (18) +HCO b (19) +HCN b (17)
1217		1323	52.0	1225	6.3	NCυ (37) + HCN b (17)
		1267	108.3	1182	33.4	HCN b (43) + CCN b (10)
1169		1218	50.4	1109	23.6	OCυ (61)

		1194	18.6	1097	12.1	CCυ (10) + HOC b (14) + HCO b (15) + HCCNτ (13) + OCCNτ (19)
		1172	6.1	1069	115.8	HCH b (28) + HCCNτ (59)
1049	1075	1114	6.2	1020	2.9	NCυ (13) + HCH b (11) + HCCNτ (37)
		1072	9.6	985	3.9	CNC b (30)
		1039	6.0	960	184.8	NCυ (10) + CCυ (42)
		1037	9.8	894	25.3	HCNCτ (82)
963		965	14.0	886	16.2	CCυ (18) + OC υ (23) + HCNCτ (23)
	830	936	55.9	833	40.0	ONO b (56) + CCN b (12)
	803	867	27.6	751	83.3	CCυ (13) + OCON γ (45)
717		803	1.8	748	110.6	CCυ (14) + OCON γ (43)
		767	17.0	693	11.6	HCCN τ (18) + CNCN τ (18)
		702	4.0	655	154.7	CCυ (16) + NC υ (19) + NCN b (28)
		664	0.7	612	28.4	CCNCτ (65)
	599	617	9.1	565	22.4	ONC b (30) + NCC b (12) + CCN b (11)
	437	545	20.0	504	48.8	CCN b (20) + OCC b (32)
		460	4.3	420	152.3	NCυ (23) + CNC b (14) + OCC b (11)
		432	4.1	396	6.3	NCυ (13) + CCN b (23) + ONC b (11) + CNC b (18)
		379	5.1	351	22.7	ONC b (12) + CCN b (48)
		328	5.5	295	199.5	HCCNτ (14) + CNNC γ (41)
		296	5.3	272	56.4	CNCb (17) + OCC b (18) + NNCC γ (15)
		264	137.3	233	12.5	NCCb (10) + HOCCτ (70)
		239	2.4	220	19.3	ONCb (11) + NCC b (43) + HOCC τ (22)
		185	12.3	169	24.6	HCCN τ (26) + NNCC γ (10) + CNNC γ (14)
		182	0.2	166	2.5	HCCNτ (42) + NNCC γ (16) + CCCN γ (15)
		138	2.8	129	2.2	CNCNτ (42) + CCNCτ (17) + OCCNτ (11) + NNCC γ (12) + CNNC γ (14)
		105	2.0	94	0.7	ONCN τ (54) + OCCN τ (25)
	74	97	2.4	90	0.5	CCNC τ (52) + NNCC γ (17)
		53	0.0	50	31.1	ONCNτ (25) + OCCN τ (11) + CCCN γ (42)
sym= symmetric, asy= asymmetric,υ= stretching, b= bending, γ= out of plane bending,τ= torsion						

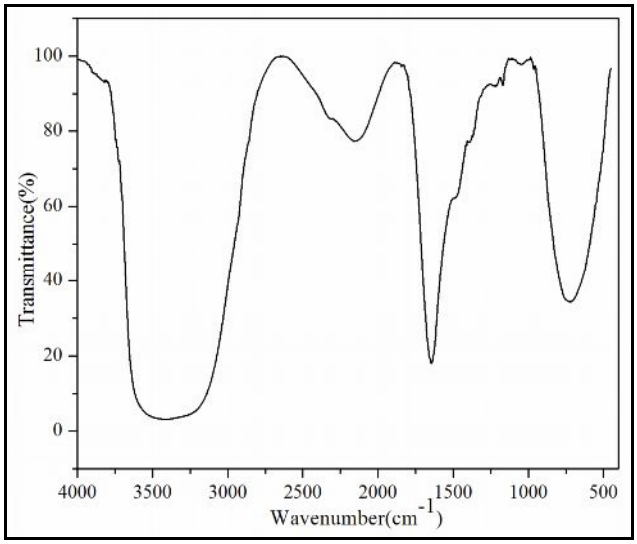

Fig 2. Experimental FTIR spectrum for Metronidazole

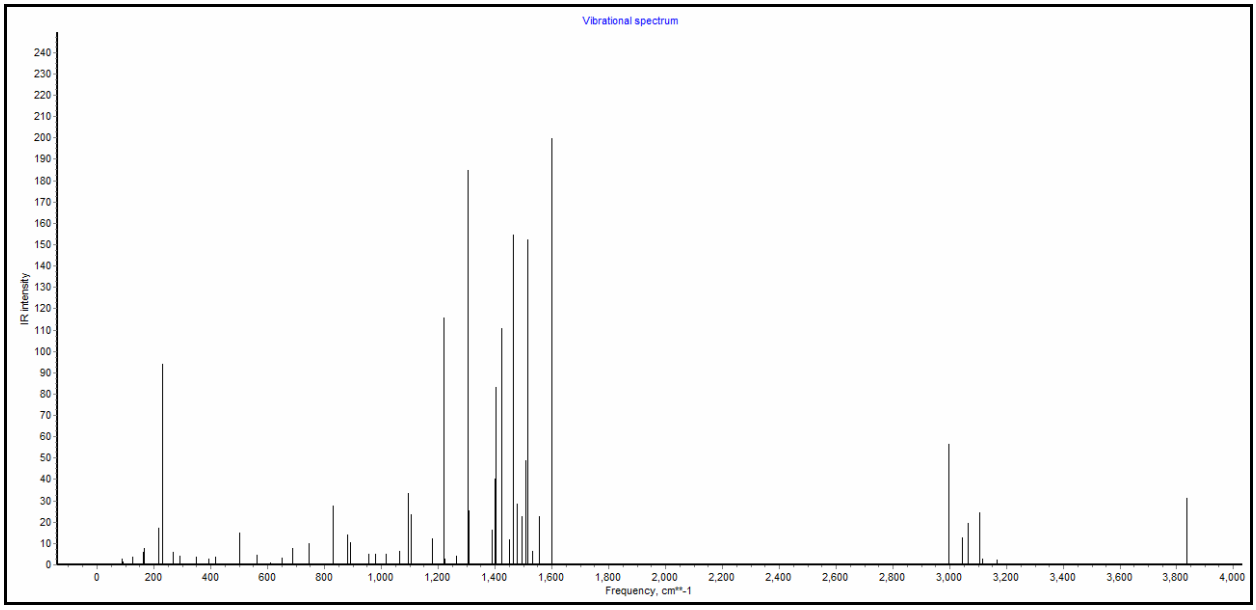

Fig 3. Simulated Vibrational spectra of Metronidazole

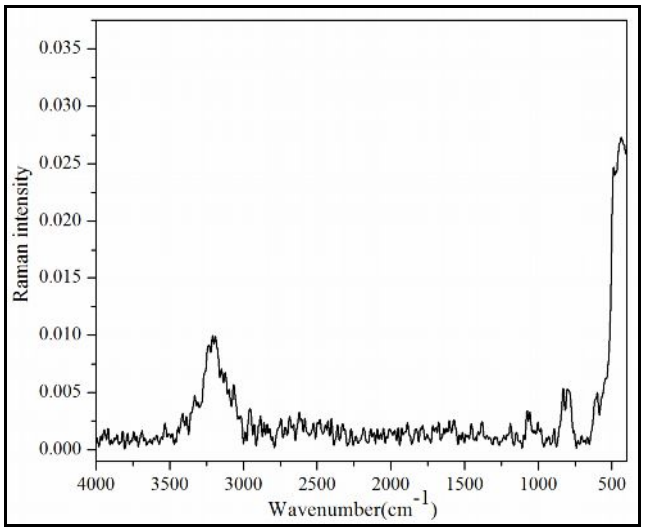

Fig 4. Experimental FT-Raman spectra for Metronidazole

O-H and C-H vibrations

The stretching vibrations of free hydroxyl group are mainly found within the region 3600-3550cm^{-1}. Hydroxyl group shows a large variation in wavenumber, intensity and bandwidth of the spectral vibrations due to presence of inter or intra molecular hydrogen bonding in the molecules [18]. The B3LYP wavenumbers 3840cm^{-1} corresponds to O-H stretching vibration and the corresponding RHF values are 4196.Arivazhagan et al [19] have also assigned B3LYP value 3628 cm^{-1} to O-H stretching.

The aromatic C-H stretching vibrations lie in the range 3100-3000cm^{-1}[20]. C-H stretching vibration is assigned to 3065, 2955, 2884cm^{-1}in FT-Raman spectrum. The corresponding B3LYP and RHF values are 3070, 3048, 3002 and 3250, 3201,3177cm^{-1} respectively. The B3LYP values are in fairly agrees with experimental values. Latha et al [21] have observed C-H stretching vibrations at 2930, 2869cm^{-1}in FTIR and at 2934, 2871cm^{-1} in FT-Raman spectra.

CH_2 vibration

The symmetric CH_2 stretching vibrations are usually observed in the region 2900-2800cm^{-1} and asymmetric CH_2 stretching vibrations appears in the range 3000-2900cm^{-1}[22]. The fundamental CH_2 vibrations due to scissoring, wagging, twisting and rocking appear in the region 1500-800cm^{-1}. The shift in wavenumber

of these bands is due to the nature of atom and molecule groups attached to the CH_2 [20]. 3208cm^{-1} in FT-Raman spectrum is assigned to CH_2 asymmetric stretching. The corresponding B3LYP and RHF wavenumbers are 3347cm^{-1} and 3177cm^{-1} respectively. Theoretical B3LYP wavenumbers are in fairly agrees with experimental wavenumbers. Ramkumaar et al [23] have observed CH_2 asymmetric stretching at 2968 in FT-Raman spectrum.

C-Nvibration

C-N stretching vibration occurs in the region 1300-800cm^{-1} [20]. The wavenumbers 1217,1049, 963cm^{-1}in FTIR and 1075, 874 cm^{-1} in FT-Raman are attributed to C-N stretching vibration. The corresponding B3LYP and RHF wavenumbes are 1225, 1020, 960cm^{-1}and 1323, 1114, 1039cm^{-1} respectively. There is a decrease in frequency because of C-N vibration mixing up with the other bending vibration. Muthu et al [24] have observed C-N stretching vibration at 976, 876 cm^{-1} in FTIR spectrum.

C-C and C-O vibrations

The ring C-C stretching vibration occurs in the region 1650-1200cm^{-1}[25]. C-C stretching vibration is observed at 1646, 963, 717cm^{-1} in FTIR spectrum. The corresponding B3LYP and RHF values are 1520, 960, 748cm^{-1} and 1661, 1039, 803cm^{-1} respectively. Ramachandran et al [26] have assigned the wavenumbers at 1021, 1010, 822, 798cm^{-1}in FTIR and 1020, 1013, 820cm^{-1} in FT-Raman spectra to C-C stretching vibration.

Generally, the C-O vibrations occur in the region 1260-1000cm^{-1} [27]. In the present study, C-O stretching vibrations are assigned to 1169cm^{-1} in FTIR, 1109cm^{-1} in B3LYP and 1218cm^{-1} in RHF. B3LYP value is in fairly agrees with experimental value. Mahalakshmi et al [28] have also assigned 1044cm^{-1}to C-O vibration in FT-Raman spectra.

4.3 UV-Vis spectral analysis

UV-Vis spectral analysis of Metronidazole has been done experimentally and theoretically. Time-dependent density functional theory (TD-DFT) is a powerful tool for investigating the static and dynamic properties of the molecules in their excited states [29]. The calculated results such as the vertical excitation energies, their molecular orbital contribution, oscillator strength (f), electronic absorption value and wavelength are reported in Table 3. The UV-Visible spectrum of Metronidazole is shown in Fig 5. Theoretical calculation predicts an intense electronic transition at 286.36 nm with an oscillator strength f=0.2213 and an electronic absorption value of4.3297 eV, involving transitions HOMO↔LUMO (76%). Another peak at 291.6 nm with an oscillator strength f=0.0021 and electronic absorption value 4.2513 involvetransitions H-6↔LUMO (19%), H-4↔LUMO (17%), H-2↔LUMO (17%), H-1↔LUMO (29%), H-5↔LUMO (5%) and H-3↔LUMO (7%). The peak at 323.1 nm with oscillator strength f=0.0003 and electronic absorption value 3.8379 corresponds to transitions H-4↔LUMO (12%), H-2↔LUMO (25%), H-1↔LUMO (51%) and H-3↔LUMO (5%). Thus, TD-DFT calculations using B3LYP/6-31++G(d,p) predict three intense electronic transitions. The observed experimental wavelength,279.5 nm corresponds to n-σ* transition.

Table 3 Experimental and calculated absorption wavelength(λ), excitation state, oscillator strength(f), electronic absorption value(eV) and transition of Metronidazole by TD-DFT method (B3LYP)

Excitation	Singlet A	Cal. Wavelength (nm)	Wave length (nm)	Oscillator Strength (f)	Electronic Absorption value (eV)	Transition
Excited state 1						
41→ 46	-0.24486	323.1		0.0003	3.8379	H-4↔LUMO (12%)
42→ 46	0.15747					H-2↔LUMO (25%)
43→ 46	-0.35290					H-1↔LUMO (51%)
44 → 46	0.50552					H-3↔LUMO (5%)

Excited state 2						
63 → 46	-0.30731	291.6		0.0021	4.2513	H-6↔LUMO (19%)
64 → 46	-0.16028					H-4↔LUMO (17%)
64 → 46	0.28787					H-2↔LUMO (17%)
63 → 46	-0.19002					H-1↔LUMO (29%)
64 → 46	0.29389					H-5↔LUMO (5%)
64 → 46	0.38385					H-3↔LUMO (7%)
Excited state 3						
45→ 46	0.61781	286.36	279.5	0.2213	4.3297	HOMO↔LUMO (76%)

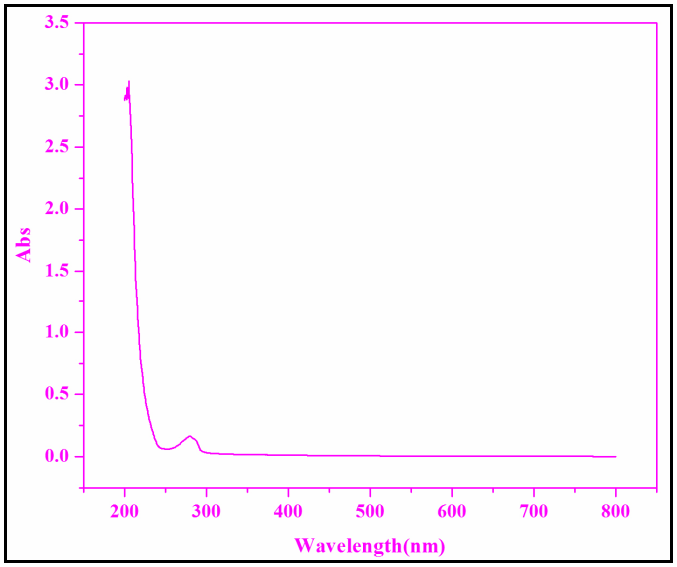

Fig 5. UV spectrum of Metronidazole

4.4 HOMO-LUMO Analysis

HOMO-LUMO orbital are the pair that lie closest in energy of any pair of orbital in the two molecules which allows them to interact most strongly. These are referred to as frontier orbital since they lie at the outermost electron boundaries of the molecules. LUMO characterizes the electrophilic component and HOMO the nucleophilic component. HOMO and LUMO play an important role in the electric and optical properties as well as in chemical reactions [28]. The energy difference between HOMO and LUMO orbital is a critical parameter in determining molecular electrical transport properties because it is a measure of electron conductivity. The positive and negative phases are represented in red and green colour respectively. LUMO is localized over the entire molecule with negative sites over C5, H17, C3, N4, N7, C6, N8, O9, H20 and positive sites over C5, H17, C3, N4, N7, C6, N8, O9 and H19. HOMO is located over the mostly in centre of the molecule. Positive sites are over C5, C6, O9, O10, H20, C3, N4 and negative sites over C1, C5, C6, O9, O10, H19, C11, C3, N4. The pictorial illustration of the frontier molecular orbitals and their respective positive and negative regions is shown in Fig 6. HOMO energy and LUMO energy are theoretically calculated to be -6.803172116 eV and -2.255025292 eV respectively. The energy gap is 4.548146824eV in B3LYP method. This energy gap characterizes the stability and explains the eventual charge transfer interactions occurring within the compound.

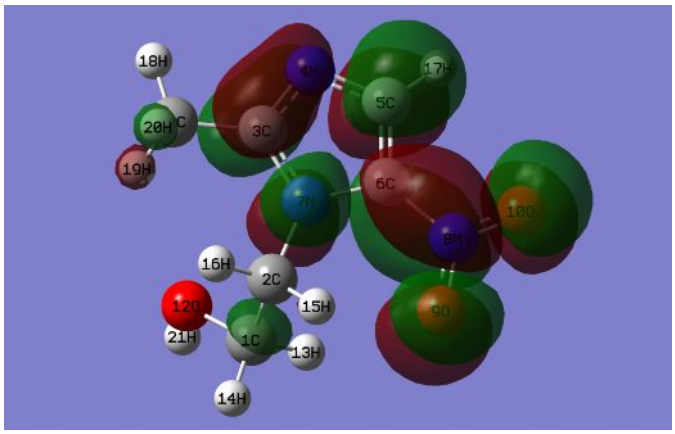

LUMO (First excited state)

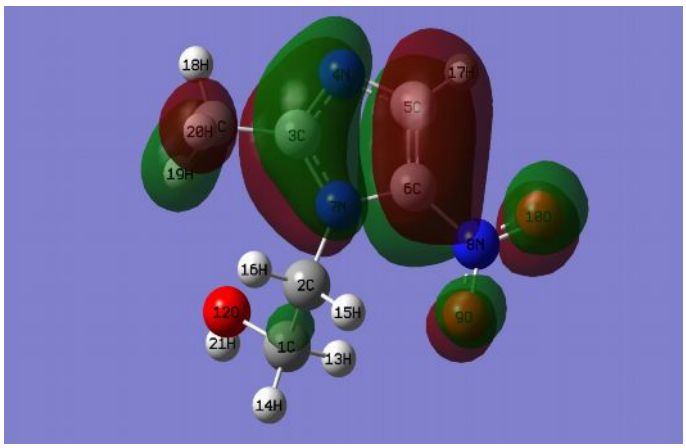

HOMO (Ground state)

Fig 6. The atomic orbital composition of the frontier molecular orbital for Metronidaz

4.5 Natural Population Analysis

The calculation of atomic charges plays a vital role in the application of quantum mechanical calculations to molecular systems. The calculated natural atomic charge values from the natural population analysis (NPA) and Mulliken Population Analysis (MPA) using DFT methods are given in Table 4. The NPA from the natural bonding orbital (NBO) method is better than MPA scheme.NPA exhibits an improved numerical stability and describes the electron distribution in compounds of high ionic character in a better way. All oxygen atoms have negative charge and all hydrogen atoms have positive charge. The oxygen atoms O9 and O10 possess large negative charges -0.43419 and -0.38573e respectively resulting in the maximum positive charge of 0.48827e on the nitrogen atom N8. H15 and H16 also have positive charge 0.27833e and 0.25093e respectively due to the electronegativity of the carbon atoms C2.The charges obtained by Mulliken and natural charge analysis are shown in Fig 7.

Table 4 Calculated atomic charges of Metronidazole by Natural Bond Orbital analysis and Mulliken Charge Analysis by B3LYP method

Atom	Natural charge	Mulliken charge
C1	-0.11194	0.052816
C2	-0.28967	-0.070882
C3	0.44761	0.479463
N4	-0.49294	-0.479912
C5	-0.01306	0.078095
C6	0.18943	0.472210

N7	-0.38672	-0.485490
N8	0.48827	0.333014
O9	-0.43419	-0.437841
O10	-0.38573	-0.403988
C11	-0.74999	-0.399205
O12	-0.77273	-0.536438
H13	0.22187	0.119348
H14	0.21219	0.098510
H15	0.27833	0.156143
H16	0.25093	0.129195
H17	0.25643	0.133666
H18	0.27509	0.150468
H19	0.27477	0.163364
H20	0.25065	0.128995
H21	0.49140	0.318470

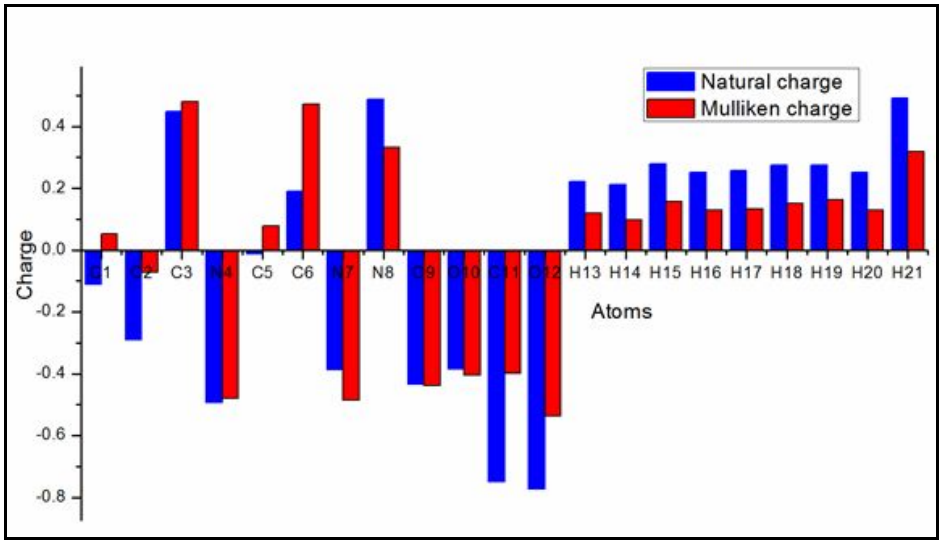

Fig. 7 Plot of Mulliken and Natural charges obtained by B3LYP/6-31G(d,p) method

4.6 Thermodynamic properties

On the basis of vibrational analysis at B3LYP/6-31G(d,p) the standard thermodynamic functions such as heat capacity, entropy and thermal energy for Metronidazole are obtained and given in Table 5. The thermodynamic data provide helpful information for further study on Metronidazole. They can be used to compute other thermodynamic energies based on the thermodynamic functions [30]. The zero point vibrational energy and total energy of the molecular structure obtained by B3LYP/6-31G (d,p) method are much lower than that obtained by RHF/6-31G(d,p) method.

Table 5:The Calculated Thermodynamic parameters of Metronidazole

Parameter	**RHF**	**B3LYP**
Zero point vibrational energy(Kcal/Mol)	111.08459	102.75956
Rotational constant (GHz)	1.30044	1.28474
	0.87600	0.85840
	0.58500	0.57283
Rotational temperatures (Kelvin)	0.06241	0.06166

	0.04204	0.04120
	0.02808	0.02749
Entropy (Cal/Mol-Kelvin)		
Total	102.796	105.873
Translational	41.318	41.318
Rotational	30.557	30.610
Vibrational	30.921	33.945
Molar capacity at constant volume		
(Cal/Mol-Kelvin)		
Total	38.446	41.383
Translational	2.981	2.981
Rotational	2.981	2.981
Vibrational	32.485	35.421
Energy (KCal/Mol)		
Total	117.844	109.967
Translational	0.889	0.889
Rotational	0.889	0.889
Vibrational	116.066	108.189

Table 6 Temperature dependence of thermodynamic properties of Metronidazole

T (K)	S (J/mol.K)	C_p (J/mol.K)	ΔH (kJ/mol)
100	303.97	88.37	5.77
200	380.36	136.04	17.07
298.15	443.08	181.46	32.63
300	444.21	182.33	32.97
400	503.01	228.13	53.52
500	558.39	268.62	78.41
600	610.44	302.26	107.01
700	659.17	329.82	138.66
800	704.75	352.54	172.82
900	747.40	371.48	209.05
1000	787.38	387.44	247.01

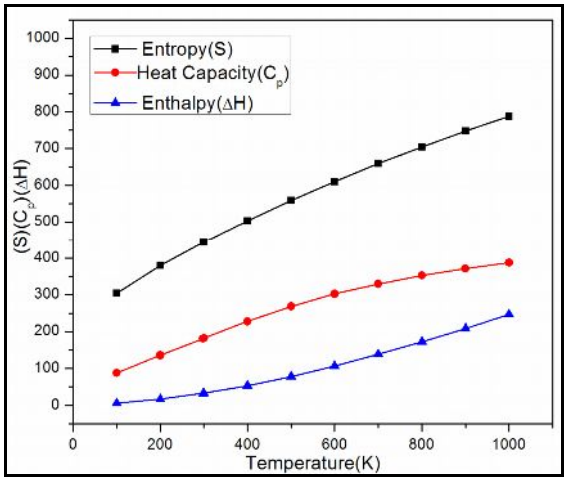

Fig 8. Correlation graph between Entropy, Heat Capacity and Enthalpy with Temperature

The thermodynamic functions increase with increase in temperature ranging from 100K to 1000K which is presented in Table 6. This is due to the fact that the molecular vibrational intensities increase with temperature. The correlation equations between entropy, heat capacity, enthalpy changes and temperature are fitted by quadratic formulae and the corresponding fitting factors (R^2) for these thermodynamic properties are 0.9997, 0.9995and 0.9996 respectively. The corresponding fitting equations are as follows and the correlation graphs are shown in Fig.8

$$S = 236.67 + 0.741T - 1.930X10^{-4}T^2 \quad R^2 = 0.9997$$
$$C_p = 27.99 + 0.594T - 2.347X10^{-4}T^2 \quad R^2 = 0.9995$$
$$\Delta H = -6.913 + 0.009T + 1.691X10^{-4}T^2 \quad R^2 = 0.9996$$

4.7 NMR spectral analysis

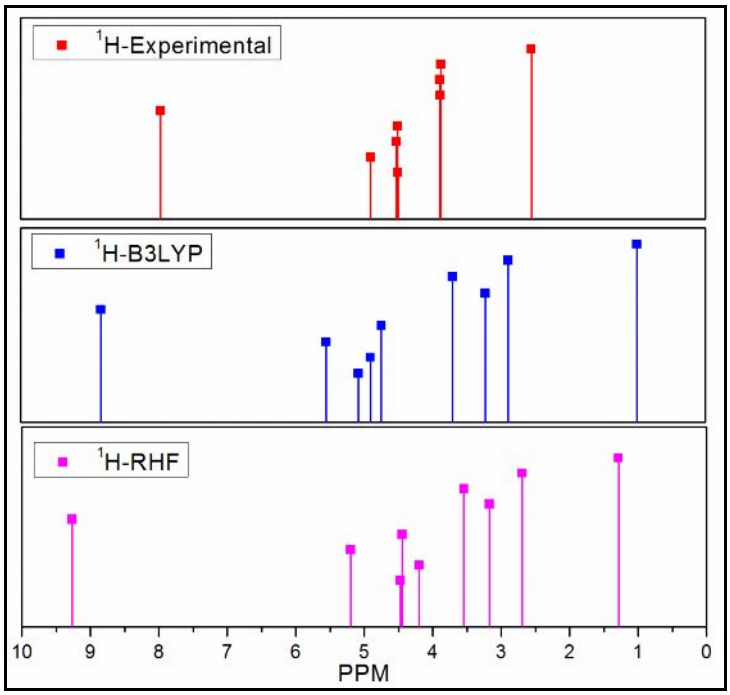

Fig 9. ^{1}H NMR Spectrum of Metronidazole (Experimental, B3LYP and RHF)

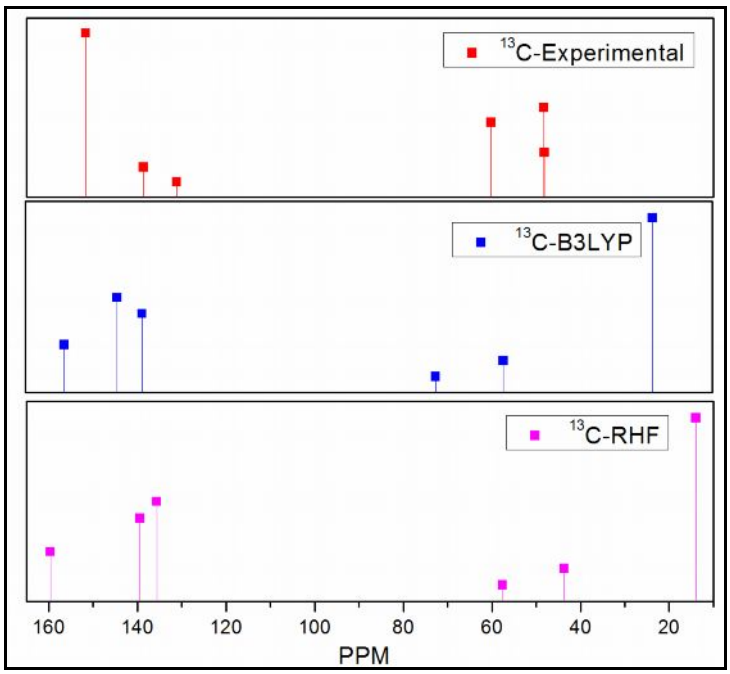

Fig 10. ^{13}C NMR Spectrum of Metronidazole (Experimental, B3LYP and RHF)

The observed 1H and 13C NMR spectra of the compound Metronidazole are given in Figs. 9 and 10, respectively.The NMR serves as a great resources in determining the structureof an organic compound by revealing the hydrogen and carbonskeleton. To furnish a definite assignment and analysis 1H and13C NMR spectra, theoretical calculations on chemical shift of Metronidazolewere done by Gauge Independent AtomicOrbital (GIAO) method at HF and B3LYP/6-31G(d,p) level. The 1H and 13C theoretical and experimental chemical shifts,isotropic shielding constants and the assignments of Metronidazoleare also given in the Table 7. Aromatic carbonsgive signals with chemical shift values from 100 to 200 ppm[31, 32]. The experimental chemical shifts of the compound occurin the range of 131.148–151.684 ppm. The chemical shift of imidazolecarbon (C3) is observed in the downfield at 151.684 ppm due to thepartial ionic nature of the imidazole group. Due to the more electronegativenitrogen atoms in ring, the chemical shift of thecarbon atoms in heterocyclic ring are set to downfield. Therefore,the chemical shift of C6 is also observed at the downfield at138.65 ppm. The C11 carbon atom is highly shielded than C2 dueto the delocalization of the electrons from N7 to theadjacent C3-C6. The chemical shifts of the benzene ring carbonatoms C3, C5 and C6 are assigned to 156.1909, 138.6839 and 144.2564 ppm, respectively. The peak observedat 48 ppm is due to solvent.

Table 7 Chemical shift (13C &1H) for Metronidazole

Atoms	Expt.	B3LYP		RHF	
	Chemical Shift	Absolute shielding	Chemical Shift	Absolute shielding	Chemical Shift
C1	60.247	127.5647	72.4206	142.3541	57.6312
C2	48.325	142.8694	57.1159	156.2684	43.7169
C3	151.684	43.7944	156.1909	40.3481	159.6372
C5	131.148	61.3014	138.6839	60.5215	139.4638
C6	138.65	55.7289	144.2564	64.3254	135.6599
C11	48.116	176.5267	23.4586	186.0225	13.9628
H13	4.490	27.5315	5.0661	28.1245	4.4731
H14	4.891	27.7048	4.8928	28.3956	4.2020
H15	4.511	27.0607	5.5369	27.3989	5.1987
H16	4.500	27.8657	4.7319	28.1498	4.4478
H17	7.957	23.7669	8.8307	23.3325	9.2651
H18	3.871	29.3813	3.2163	29.4226	3.1750
H19	3.882	28.9037	3.6939	29.0526	3.5450
H20	3.861	29.7180	2.8796	29.9038	2.6938
H21	2.544	31.5984	0.9992	31.3102	1.2874

The chemical shifts for the ^{1}H atoms are quite low, as the hydrogen atoms attached to nearby electron-withdrawing atom and group can decrease the shielding. The protons have chemical shifts experimentally in the range 2.544 ppm to 7.957 ppm which is in fairly agrees with B3LYP theoretical values.The experimental and theoretical NMR spectrum of ^{1}H and ^{13}C are shown in Figs. 9 and 10.

5. Conclusion

The molecular geometry of the molecule in the ground state has been calculated by using RHF and DFT (B3LYP) methods with 6-31G(d,p) basis set. Several thermodynamical parameters were obtained and analyzed with RHF and DFT methods using the same basis set. UV-Visible spectral analysis of the molecule was also carried out. The HOMO-LUMO energy gap helped in analyzing the chemical reactivity of the molecule. Atomic charges of the molecule were studied by both the RHF and DFT methods. The ^{1}H and ^{13}C NMR chemical shifts were calculated and compared with the experimental results. On comparing the experimental results with the theoretically predicted values, it was found that the B3LYP method was more accurate, proving that DFT is a reliable method for molecular vibrational analysis.

Acknowledgement

The authors would like to acknowledge the Sophisticated Analytical Instrument Facility, Indian Institute of Technology, Madras, India, for providing the facilities for spectral measurements.

References

1. M.E.Wol, John Wiley and Sons, "Text book of Burgers Medicinal Chemistry", fourth ed., New York, 979 2(4) (2009) 865-868.
2. C.Coser, L.Julon, Ann. inst. Pasteur, 96 (1958) 238.
3. D.I.Edwards., J.antimicrob.chemother, 31 (1993) 9.
4. C.Cosar, C.Cusan, R.Horclosis, R.M.Jacob, J.Robert, J.STchelitche, R.Vapure, Arzneim –Forsch, 16 (1966) 23.
5. S.J.Powell, I. McLeod, A.J. Wilmot, R. Elsdon- Dew, Lancet, 2, 1329. (1969)
6. S.J.Powell, Bull. N.Y. Acad.Med., 47 (1971) 469.
7. R.B.Khambatta, Ann.Trop. Med. Parasitol, 62 (1968) 139.
8. Indian Pharmacopoeia, Controller of Publications, New Delhi, 2 (1996) 764.
9. British Pharmacopoeia, Her Majesty's Stationery Office, London, 2 (2003) 1257.
10. The United States Pharmacopoeial Convention, Rockville, MD, The United States Pharmacopoeia 24th edn. The National Formulary, 19 (2000) 1104.
11. P. D. Panzade, K. R. Mahadlik, East Pharm, 43 (2000) 115.
12. P. Nagaraja, K. R. Sunitha, R. A. Vasantha, H. S. Yathirajan, J. Pharm. Biomed. Anal, 28 (2002) 527.
13. T. Saffaj, A. Charrouf, Y. Abourriche, A. abboud, M. B. Bennamara, Formaco, 59 (2004) , 843.
14. D. M. Joshi, A. P. Joshi, J. Indian. Chem. Soc.,74 (1997) 585.
15. M. J. Frisch, G. W. Trucks, H. B. Schlegel, G. E. Scuseria, M. A. Robb, J. R. Cheeseman, G. Scalmani, V. Barone, B. Mennucci, G. A. Petersson, H. Nakatsuji, M. Caricato, X. Li, H. P. Hratchian, A. F. Izmaylov, J. Bloino, G. Zheng, J. L. Sonnenberg, M. Hada, M. Ehara, K. Toyota, R. Fukuda, J. Hasegawa, M. Ishida, T. Nakajima, Y. Honda, O. Kitao, H. Nakai, T. Vreven, J. A. Montgomery, Jr., J. E. Peralta, F. Ogliaro, M. Bearpark, J. J. Heyd, E. Brothers, K. N. Kudin, V. N. Staroverov, R. Kobayashi, J. Normand, K. Raghavachari, A. Rendell, J. C. Burant, S. S. Iyengar, J. Tomasi, M. Cossi, N. Rega, J. M. Millam, M. Klene, J. E. Knox, J. B. Cross, V. Bakken, C. Adamo, J. Jaramillo, R. Gomperts, R. E. Stratmann, O. Yazyev, A. J. Austin, R. Cammi, C. Pomelli, J. W. Ochterski, R. L. Martin, K. Morokuma, V. G. Zakrzewski, G. A. Voth, P. Salvador, J. J. Dannenberg, S. Dapprich, A. D. Daniels, O. Farkas, J. B. Foresman, J. V. Ortiz, J. Cioslowski, and D. J. Fox, Gaussian, Inc., Wallingford CT, 2009.
16. H. B. Schlegel, Journal of Computational Chemistry, 3(2) (1982) 214–218.
17. L.E.Sutton, The inter atomic bond and bond angles in molecules and ions, (Chemical Society) London, 1956.
18. B. Smith, Infrared Spectral Interpretation: A Systematic Approach, CRC, Washington, DC, 1999.
19. M. Arivazhagan, D. Anitha, Spectrochimica Acta Part A, 104 (2013) 451-460.
20. M. Silverstein, G.C. Basseler, C. Morill, "Spectrometric Identification of Organic Compunds", Wiley, New York, 1981.
21. B. Latha, S. Gunasekaran, S. Srinivasan, G.R. Ramkumaar, Spectrochimica Acta Part A, 132 (2014) 375-386.
22. K. Furic, V. Mohack, M. Bonifacic, J. Mol. Struct. 267 (1992) 39-44.
23. G.R. Ramkumaar, S. Srinivasan, T.J. Bhoopathy, S. Gunasekaran, B. Prameena, J. Mol. Struct., 1059 (2014) 185 -192.
24. S. Muthu, S. Renuga, Spectrochimica Acta Part A, 118 (2014) 683 – 694.
25. L.J. Bellamy, The Infrared Spectra of Complex Molecule, 3rd Ed. Wiley, NewYork, 1975.
26. G. Ramachandran, S. Muthu, S. Renuga, Spectrochimica Acta Part A, 107 (2013) 386 – 398.
27. G. Varsanyi, Vibrational Spectra of Benzene Derivatives, Academic Press, New York,
a. 1969.
28. G. Mahalakshmi, V. Balachandran, Journal of Molecular Structure, 1063 (2014) 109-122.
29. A. Dreuw, M.Head-Gordon, Chem. Rev., 105 (2005) 4009 - 4037.
30. R. Zhang, B. Dub, G. Sun, Y.Sun, Spectrochimica Acta Part A, 75 (2010) 1115-1124.
31. H.O. Kalinowski, S. Berger, S. Braun, Carbon-13 NMR Spectroscopy, John Wiley & Sons, Chichester, 1988.
32. K. Pihlaja, E. Kleinpeter (Eds.), Carbon-13 Chemical Shifts in Structural and Sterochemical Analysis, VCH Publishers, Deerfield Beach, 1994.

*****

*****